Bioresource Technology 394 (2024) 130226

Contents lists available at ScienceDirect

Bioresource Technology

journal homepage: www.elsevier.com/locate/biortech

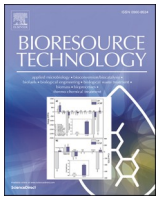

Intensification of moisture separation in the pulp convective drying process with ultrasound-assisted method

Lingbo Kong [a,b,*], Jiahao Li [a], Wolfgang Eichhammer [b,c]

[a] Department of Mechanical and Electrical Engineering, Shaanxi University of Science and Technology, 710021 Xi'an, China
[b] Fraunhofer Institute for Systems and Innovation Research ISI, 76139 Karlsruhe, Germany
[c] Copernicus Institute of Sustainable Development, Utrecht University, 3584 CB Utrecht, Netherlands

HIGHLIGHTS

- Ultrasound-assisted drying (UAD) could intensify the moisture separation in pulp drying process.
- The drying time was shortened by 26 %~42 % as a result of UAD intensification.
- Drying at 55 °C and 60 W led to the minimized energy consumption with UAD.
- The Page model was found to be the best for predicting the pulp drying kinetics.
- No significant differences in drying rates were observed when the moisture ratio was below 0.43.

ARTICLE INFO

Keywords:
Ultrasound
Moisture separation
Intensification
Convective drying
Pulp

ABSTRACT

Traditional pulp convective drying (CD) is time-consuming and energy-intensive. This study aimed to assess the drying performance of pulp using ultrasound-assisted drying (UAD) and compared it with CD to intensify moisture separation. UAD was found to be fast and efficient with high effective moisture diffusivity of $2.77 \times 10^{-10} \sim 3.20 \times 10^{-10}$ m^2/s, low activation energy of 20.2 kJ/mol, and short drying time of 21.0 ~ 16.5 min. It demonstrated that applying ultrasound could promote moisture separation with 26 %~42 % reductions in drying time and 42 %~22 % savings in energy consumption. The constant rate period was not presented and no significant differences in drying rates were observed when the moisture ratio was below 0.43 under the investigated conditions. The kinetics modeling results indicated that the Page model was the best to predict the pulp drying kinetics for both methods. It may lead to an alternative efficient approach for decarbonizing the drying process in pulp and paper production.

1. Introduction

Cellulose pulp is one of the main raw materials used for making paper products. In order to facilitate storage and transportation, the wet pulp generally has to be dried or the water has to be separated from the wet pulp during the production process in the non-integrated pulp and paper mills. The dried pulp is usually in the form of pulp board, also named market pulp, for transporting it conveniently. Although using market pulp can reduce the equipment investment and energy costs for the stand-alone paper mills, it has extended the production chain of the paper industry and increased additional costs and environmental loads for the paper industry. With increasing awareness of energy conservation and carbon mitigation, many efforts have to be undertaken for improving the efficiency of the pulp drying process.

Convective drying (CD) is the most common technology that is applied broadly for separating moisture from moist porous materials, such as pulp or paper, fabric, and food products due to the simplicity of dryer construction, easy operation, and low investment cost. Nevertheless, there are also drawbacks for this traditional moisture separation technology, e.g., long drying time, low drying efficiency, high energy consumption, and significant quality degradation. To overcome these disadvantages, some emerging technologies, such as infrared drying (Huang et al., 2021), microwave drying (Behera and Balasubramanian, 2021), electrohydrodynamic drying (Yang and Yagoobi, 2022), ultrasound-assisted drying (UAD) (Yao et al., 2020), and hybrid drying (Zhang et al., 2023), have been investigated and developed to intensify the moisture and/or heat transfer in the moisture separation process of

* Corresponding author at: Department of Mechanical and Electrical Engineering, Shaanxi University of Science and Technology, 710021 Xi'an, China.
E-mail address: lbkong@sust.edu.cn (L. Kong).

https://doi.org/10.1016/j.biortech.2023.130226
Received 16 November 2023; Received in revised form 17 December 2023; Accepted 17 December 2023
Available online 18 December 2023

Nomenclature

a, b, c	Model constants
D_{eff}	Effective moisture diffusivity (m^2/s)
D_0	Pre-exponential factor of the Arrhenius equation (m^2/s)
DR	Drying rate (g water/(g fiber·min))
E_a	Activation energy (J/mol or W/g)
k	Slope
L	Thickness (m)
m	Mass (g)
M	Moisture content (g water/g fiber)
M_w	Molar mass of the water (18 g/mol)
MR	Moisture ratio
$\overline{MR}$	Average moisture ratio
N	Number of observations
n	Number of constants
P	Ultrasonic power (W)
R	General gas-constant (8.314 J/(mol·K))
R^2	Coefficient of determination
$RMSE$	Root mean square error
SEC	Specific energy consumption (kWh/kg)
T	Temperature (K)
TEC	Total energy consumption (kWh)
t	Drying time (s or min)
χ^2	Reduced chi-square

Subscripts

a	Activation energy
aver	Average
CD	Convective drying
cf	Centrifugal fan
d	Drying/Dried
e	Equilibrium
eff	Effective moisture diffusivity
eh	Electronic heater
exp,i	The i^{th} experimental value
i	Initial
per,i	The i^{th} predicted value
UAD	Ultrasound-assisted drying
UR	Ultrasound reduction
UTP	Ultrasonic thermal effect
ug	Ultrasonic generator

moist porous material. The infrared drying and microwave drying usually caused local overheating owing to uneven moisture distribution within the material which degrade the product quality. However, as an efficient alternative, UAD could accelerate moisture separation with increased energy efficiency through mechanical effects and sponge effect, which reduce both external and internal resistance of mass transfer, while also preserving the quality of the materials being dried.

Recently, UAD has been proved to be a promising drying technique for intensifying the moisture and heat transfer while preserving the quality of the products being dried (Zhang and Abatzoglou, 2020). It has been widely utilized in the drying of fruits, vegetables, and food products with substantially reduces drying time and energy consumption, either with airborne ultrasound or direct contact ultrasound method (Fan et al., 2017; Huang et al., 2020). The effect of ultrasound on the drying process and quality aspects of food products were reviewed or studied in detail in the literature (Siucińska and Konopacka, 2014; Tayyab Rashid et al., 2022). A positive effect of application UAD was always obtained from available studies that not only accelerated drying rate but also improved energy efficiency. Based on the efficient enhancement of moisture separation, the researchers at Oak Ridge National Laboratory developed the direct contact ultrasonic fabric drying technique to intensify the fabric drying (Dupuis et al., 2019; Peng et al., 2017a). The contact ultrasonic fabric drying was based on direct mechanical coupling between mesh piezoelectric transducers and wet fabric, which results in the moisture as a fine mist of very small droplets and then ejected from the wet fabric. With this new technique, the fabric drying kinetics under different conditions were investigated experimentally and analytically by Peng and Moghaddam (2021). They also studied the ultrasonic drying performance of various fabrics and found that an order of magnitude decreases in energy consumption compared with a typical electric resistance dryer, and five times lower than the latent heat of vaporization at moisture content greater than 20 % (Peng et al., 2017b). Li and Chen (2017) applied UAD to enhance fabric drying process and observed the nonlinear relationship between ultrasound power and drying rate. As a result of the demonstrated great potential for intensification of food and fabric drying process with ultrasound, it has been conjectured that UAD could also use for improving the drying efficiency of pulp or paper products. As of now, the group led by Prof. Yagoobi from Worcester Polytechnic Institute (WPI), for the first time, conducted experimental and numerical researches on UAD of paper products and confirmed the effectiveness of ultrasound on intensifying the paper drying process with obvious enhancement of drying rate and energy efficiency (Asar et al., 2022; O'Connor et al., 2023). The impacts of initial moisture content, thickness, and refining condition of paper samples were studied in the UAD process (O'Connor et al., 2023). Besides, the effect of applying ultrasound transducers in a multicylinder dryer section on paper drying energy efficiency was also illustrated numerically (Asar et al., 2022). Although the employed ultrasound was produced by a piezoelectric transducer at 3 W of load power and 1.7 MHz frequency in their experiments, the results provided basic data toward fundamental understanding of the application of ultrasound for paper drying.

In this work, the dried sample is expanded to pulp, the raw biomaterial for papermaking. In addition to applied different contact UAD method from WPI, the condition of process variables, such air velocity and air temperature, on convective drying process will also be considered for enhancing the pulp drying process, namely the UAD is conducted in the traditional pulp convective process. It was reported the magnitude of ultrasound improvement effect on drying process was largely dependent on the process variables (Huang et al., 2020). Additionally, the effect of ultrasound power levels on drying process was also studied in the current work because an energy intensity threshold has been observed in the intensification of mass transfer processes with UAD. For example, Cárcel et al. (2007) found that the enhanced dehydration effects were not obvious at the lower levels of ultrasonic intensity (3.6 and 8.0 W/cm^2) for static treatment of apples slices until the intensity increased to 10.8 W/cm^2 and confirmed the existence of an intensity threshold above which the effect of ultrasound on moisture separation were significant. García-Pérez et al. (2009) also indicated that the influence of ultrasonic power on carrot drying was not observed until the power density exceeded a minimum value (8 ~ 12 kW/m^3), and the drying time was reduced by 32 % when the ultrasonic density increased from 4 to 37 kW/m^3.

To the best of our knowledge, we did not find literature available so far on evaluating specifically the existence of a threshold regarding intensification pulp and paper products drying with UAD. For a better understanding of the effects linked to the use of ultrasonic power and air temperature, it is necessary to investigate its possible limitations when applied for intensifying pulp drying process. This study aims to validate the feasibility of UAD for intensifying the convective drying process of pulp or paper products. The impacts of hot-air temperature and ultrasonic power on the pulp drying kinetics were also investigated in the

present work. Then, mathematical modeling of pulps in CD and UAD processes was carried out to explore the thin-layer drying kinetics. The effective moisture diffusivity and activation energy for CD and UAD processes were then determined. The contribution of this work can provide insights and further understanding of the application of UAD for separating water from pulp and paper products more efficiently, e.g., shorter drying time and lower energy consumption.

2. Materials and methods

2.1. Preparation of pulp samples

The experimental material used in this study was an unbleached kraft pulp imported from Canada and stored in plastic bags at room temperature. The original size of the pulp board was 850 mm × 800 mm × 1 mm. Before the drying experiments, part of the original pulp was cut into a large number of square samples with a side length of 80 mm and a weight of about 5.00 ± 0.10 g, which were soaked in purified water for 24 h after having determined the average initial weight. Absorbent papers were used to remove the excess water on the surface of wet pulp. After this step, samples were put it into sealed bags to protect them against moisture loss. To determine the initial moisture content of the pulp, three wet samples were weighed and dried in an oven at 105 ℃ for 24 h. The obtained initial moisture content of the wet pulp was 1.50 ± 0.01 g water/g fiber.

2.2. Drying methods

2.2.1. Convective drying (CD) method

The CD experimental setup was mainly composed of a drying chamber, centrifugal fan (150FLJ7, China), electric heater (PCT constant temperature heater, China), temperature controller (W141, China), hot wire anemometer (Testo 405i, Germany), and electronic balance (HZF-A, America) as shown in Fig. 1. The convective drying experiments of pulp were carried out at hot-air temperatures of 45, 55, and 65 ℃. The hot-air velocity was kept at 3 m/s in the experiment. When the hot-air temperature and velocity reached the specified conditions and kept steady, the wet pulp samples were placed on the stainless-steel plate in the drying chamber to be dried. The digital balance (0.01 g accuracy) was used to measure the weight of wet pulp every 90 s until no mass changed. All the drying experiments were replicated three times at each hot-air temperature.

2.2.2. Ultrasound-assisted drying (UAD) method

Based on the CD experimental setup, an ultrasonic generator (THD-T1, China), ultrasonic transducer (25K100W, China), and ultrasonic vibration plate with 2 mm thickness were constructed for the UAD experiment. A schematic diagram of the experimental setup is presented in Fig. 1. It was firstly preheated for 20 min to ensure uniform drying temperature at the velocity of 3 m/s. Then the wet sample was placed on the ultrasonic vibration plate in the drying chamber before turn on the ultrasonic generator and the ultrasonic frequency was set at 22.6 kHz. The drying experiments were carried out under ultrasonic power of 30, 60, and 90 W. The remaining approach was identical to the CD experiment.

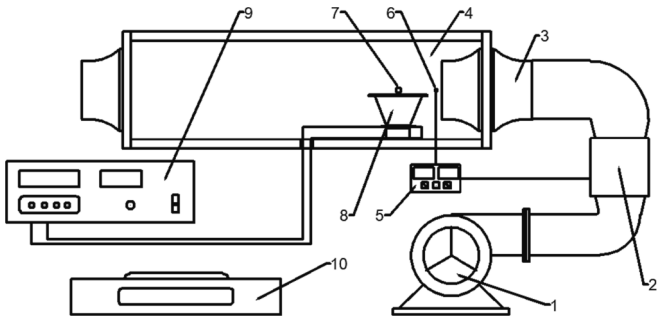

Fig. 1. Schematic diagram of the pulp drying experimental setup.

2.3. Mathematical modeling

The dry basis moisture content (M, g water/g fiber) and drying rate (DR, g water/(g fiber·min)) of the pulp can be defined as follows in Eq. (1) and Eq. (2):

$$M = \frac{m_i - m_d}{m_d} \tag{1}$$

$$DR = \frac{M_{t1} - M_{t2}}{t_1 - t_2} \tag{2}$$

where m_i and m_d are the initial mass and absolutely dried mass of the pulp (g), t_1 and t_2 are the drying time (min), M_{t1} and M_{t2} are the moisture content of the pulp at time t_1 and t_2 (g water/g fiber).

For modeling the drying kinetics of various materials, the thin-layer models were widely utilized and can be found from the literature (Behera and Balasubramanian, 2021; Buzrul, 2022; Luo et al., 2015; Sun et al., 2017; Zhu et al., 2021). For example, Luo et al. (2015) reported that the relationship between the moisture ratio (MR) and different influencing factors (ultrasonic power, ultrasonic radiation distance, and hot-air temperature and velocity) for UAD of carrots followed the Page model. Sun et al. (2017) revealed that the Midilli model described satisfactorily the moisture ratio with the ultrasonic power and hot-air temperature in the CD and UAD processes of sludge. In this work, six mathematical models were chosen to fit the pulp drying kinetics as shown in Table 1. The dimensionless moisture ratio (MR) of the pulp during the drying process was calculated by Eq. (3):

$$MR = \frac{M_t - M_e}{M_i - M_e} \tag{3}$$

where M_t is the moisture content (g water /g fiber) at time t, M_i is the initial moisture content (g water/g fiber) and M_e is the equilibrium moisture content (g water/g fiber). The equilibrium moisture content can be ignored in the MR calculation since it is very small.

The coefficient of determination (R^2), reduced chi-square value (χ^2), and root mean square error ($RMSE$) were used to evaluate the quality of fit for each model. The value of R^2 determines the fitting ability of the models, and it is required to reach 1 for the best results. On the contrary, $RMSE$ and χ^2 represent the deviation between the theory and experiment, showing the best results of fitting when the values of $RMSE$ and χ^2 reach 0. The equations of R^2, χ^2, and $RMSE$ were Eq. (4), Eq. (5), and Eq. (6), respectively.

Table 1
Mathematical models applied to the pulp drying kinetics.

Model name	Model equation	References
Lewis	$MR = \exp(-kt)$	(Buzrul, 2022; Peng and Moghaddam, 2021; Sun et al., 2017; Zhu et al., 2021)
Page	$MR = \exp(-kt^n)$	(Behera and Balasubramanian, 2021; Buzrul, 2022; Sun et al., 2017; Zhu et al., 2021)
Logarithmic	$MR = a\exp(-kt) + c$	(Buzrul, 2022; Peng and Moghaddam, 2021; Sun et al., 2017)
Henderson and Pabis	$MR = a\exp(-kt)$	(Buzrul, 2022; Peng and Moghaddam, 2021; Sun et al., 2017; Zhu et al., 2021)
Wang and Singh	$MR = 1 + at + bt^2$	(Buzrul, 2022; Sun et al., 2017; Zhu et al., 2021)
Midilli et al.	$MR = a\exp(-kt^n) + bt$	(Buzrul, 2022; Sun et al., 2017; Zhu et al., 2021)

$$R^2 = 1 - \frac{\sum_{i=1}^{N}\left(MR_{\exp,\ i} - MR_{\mathrm{pre},i}\right)^2}{\sum_{i=1}^{N}\left(\overline{MR}_{\exp,i} - MR_{\mathrm{pre},i}\right)^2} \tag{4}$$

$$\chi^2 = \frac{\sum_{i=1}^{N}\left(MR_{\exp,i} - MR_{\mathrm{pre},i}\right)^2}{N-n} \tag{5}$$

$$RMSE = \sqrt{\frac{\sum_{i=1}^{N}\left(MR_{\exp,i} - MR_{\mathrm{pre},i}\right)^2}{N}} \tag{6}$$

where $MR_{\exp,i}$ is the i^{th} experimentally observed moisture ratio, $MR_{\mathrm{pre},i}$ is the i^{th} predicted moisture ratio, $\overline{MR}_{\exp,i}$ is the i^{th} experimentally average moisture ratio, N is the number of observations, and n is the number of the constants.

2.4. Calculation of effective moisture diffusivity and activation energy

During ultrasound-assisted convective drying processes, the moisture transport properties can be lumped into the effective moisture diffusivity (D_{eff}), which is affected by pulp properties, moisture content, drying temperature and air velocity, as well as ultrasonic power. The effective moisture diffusivity is a key indicator that presents possible mechanism of moisture separation in terms of liquid diffusion, vapor diffusion, surface diffusion and capillary flow and so on (Sun et al., 2017). Assuming internal moisture separation as the dominant mechanism, the variation of moisture content with drying time can be expressed in the form of Eq. (7) according to Fick's second law of diffusion.

$$\frac{\partial M}{\partial t} = D_{\mathrm{eff}}\nabla^2 M \tag{7}$$

where D_{eff} is the effective moisture diffusivity (m^2/s) and t is the drying time (s).

In most situations, the pulp is assumed as one-dimensional with uniform initial moisture content. The solution of Eq. (7) for a plane sheet is as follows (Ertekin and Firat, 2015; Onwude et al., 2016):

$$MR = \frac{8}{\pi^2}\sum_{n=0}^{\infty}\frac{1}{(2n+1)^2}\exp\left[-\frac{(2n+1)^2\pi^2 D_{\mathrm{eff}}}{L^2}t\right] \tag{8}$$

where L is the thickness of the pulp board (m).

For a long drying time of the pulp, the solution of Fick's equation can be simplified solved by the first term of Eq. (8). Thus, the first term of Eq. (8) can be extracted and then linearly written in the form of Eq. (9):

$$\ln(MR) = \ln\left(\frac{8}{\pi^2}\right) - \frac{\pi^2 D_{\mathrm{eff}}}{L^2}t \tag{9}$$

Thus, the value of D_{eff} could be obtained from the slope k_{eff} of the straight line obtained from plotting ln (MR) versus t using Eq. (10).

$$D_{\mathrm{eff}} = -\frac{L^2}{\pi^2}k_{\mathrm{eff}} \tag{10}$$

where k_{eff} is the slope of logarithm MR versus drying time and can be obtained by linear regression analysis.

The activation energy, E_a, is the smallest energy required to overcome an energy barrier and start a process. In the CD process, the activation energy ($E_{a,CD}$, J/mol) was expressed by the Arrhenius equation (Behera and Balasubramanian, 2021; Ozuna et al., 2014):

$$D_{\mathrm{eff}} = D_0\exp\left(-\frac{E_{a,CD}}{RT}\right) \tag{11}$$

where D_0 is the pre-exponential factor of the Arrhenius equation (m^2/s), R is the general gas-constant (8.314 J/(mol·K)), and T is the absolute temperature (K). Then, transforming Eq. (11) into a linear form by applying logarithm on both sides (Eq. (12)):

$$\ln(D_{\mathrm{eff}}) = \ln(D_0) - \frac{E_{a,CD}}{RT} \tag{12}$$

The activation energy, $E_{a,CD}$ (J/mol), could be determined from the slope k_a by Eq. (13).

$$E_{a,CD} = -Rk_a \tag{13}$$

where k_a is the slope of straight line on the plot of ln (D_{eff}) and $1/T$.

In the UAD process, the ultrasonic thermal effect that results in the actual drying temperature of samples is slightly higher than the theoretical drying temperature, and the amount of temperature rise caused by different ultrasonic power is different. As the UAD process under different ultrasonic power levels is not an isothermal process, the modified form of the Arrhenius equation, Eq. (14), was applied to calculate the activation energy (Behera and Balasubramanian, 2021; Beigi and Torki, 2021).

$$D_{\mathrm{eff}} = D_0\exp\left(-m\frac{E_{a,UTP}}{P_{ug}}\right) \tag{14}$$

where P_{ug} is the ultrasonic generator power (W), and $E_{a,UTP}$ is the part of activation energy that is provided by the ultrasonic thermal effect in the UAD process (W/g). The reduced activation energy by the application of ultrasound can be calculated by Eq. (15), in which the contribution of thermal effect with ultrasound to drying efficiency was supposed to 17 % (Kowalski and Mierzwa, 2015).

$$E_{a,UR} = \frac{E_{a,UTP}M_w t_{aver}}{17\%} \tag{15}$$

where $E_{a,UR}$ is the activation energy reduced by the application of ultrasound (J/mol), M_w is the molar mass of water (18 g/mol), and t_{aver} is the average drying time per gram of water in the UAD process (s). Therefore, the activation energy of UAD ($E_{a,UAD}$, J/mol) can be expressed as the difference between the activation energy of CD and the activation energy reduced by the convection drying process due to ultrasonic enhanced effect and expressed with Eq. (16).

$$E_{a,UAD} = E_{a,CD} - E_{a,UR} \tag{16}$$

2.5. Calculation of energy consumption

To compare and analyze energy consumption difference between CD and UAD, the total energy consumption (*TEC*, kWh) is used to calculate the total energy use in the drying process. During pulp drying process, *TEC* includes energy consumption of electronic heater, ultrasonic generator, and centrifugal fan. Meanwhile, since the evaporations in each experiment varies somewhat, the specific energy consumption (*SEC*, kWh/kg) is generally used to evaluate the unit energy consumption for evaporating 1 kg of water during the different drying processes.

The *TEC* in kWh and *SEC* in kWh/kg can be determined by Eqs. (17) and (18).

$$TEC = (P_{eh} + P_{cf} + P_{ug})t \tag{17}$$

$$SEC = \frac{TEC}{m_i - m_d} \tag{18}$$

where P_{eh} is the effective power output of the electric heater (kW), P_{cf} is the effective power output of the centrifugal fan (kW), and P_{ug} is the effective power output of the ultrasonic generator (kW). P_{ug} equals to zero in the CD process.

3. Results and discussion

3.1. Convective drying (CD) results and discussion

3.1.1. Effect of drying temperature on CD kinetics

The plot of moisture ratio with drying time at different temperatures in the convective drying has been presented in Fig. 2a. It was observed that the drying time of CD was 48.0 min at the hot-air temperature of 45 ℃, and decreased to 28.5 and 25.5 min at hot-air temperatures of 55 and 65 ℃. Although the temperature increased by 10 ℃ for each experiment, only 11 % of drying time was saved when the temperature rose to 65 from 55 ℃, while it was 41 % as the temperature rose to 55 from 45 ℃. In addition, the average drying rates were 0.0298, 0.0502, and 0.0559 g water/(g fiber·min) at hot-air temperatures of 45, 55, and 65 ℃, respectively. As expected, the average drying rate was enhanced with increasing hot-air temperature and consequently reduced the drying time. This is attributed to the improvement of the driving force for moisture transport between the pulp surface and the dry medium. At the same time, the rapid evaporation of moisture on the pulp surface also enlarges the moisture concentration difference between the interior and the surface of the dried pulp. To keep the pulp surface in a wet state, the internal moisture will quickly diffuse to the surface and then evaporate. The improvement of the diffusion rate of internal moisture and the evaporation rate of surface moisture causes the intensification of the whole drying process as hot-air temperature rises.

In addition to the warm-up rate period, both a constant rate period and falling rate period were observed in the pulp CD experiments at 45 and 55 ℃, as shown in Fig. 2b. At the constant rate drying period, the moisture separation rate from inside of the pulp by liquid diffusion can meet the requirements of the surface evaporation rate so that the water will be evaporated constantly from the pulp surface. When the *MR* decreases to 0.62, the drying process enters the falling rate period. At this stage, the drying rate is determined by internal moisture evaporation and diffusion. Namely, the moisture evaporated internally and then diffused to the pulp surface. The drying rate began to decline due to increased absorption energy requirement and longer diffusion pathway from inside to the surface. As drying proceeds, the vapor diffusion resistance also increases which resulted in lowering the drying rate. However, it should be noted that the constant rate period was not very extended at 65 ℃, since the waterfront recedes into the pulp quickly at a higher moisture separation rate. After the maximum drying rate was reached at the *MR* of 0.8, the drying rate started to decrease until it was close to zero. Therefore, not all the CD processes will present a constant rate drying period.

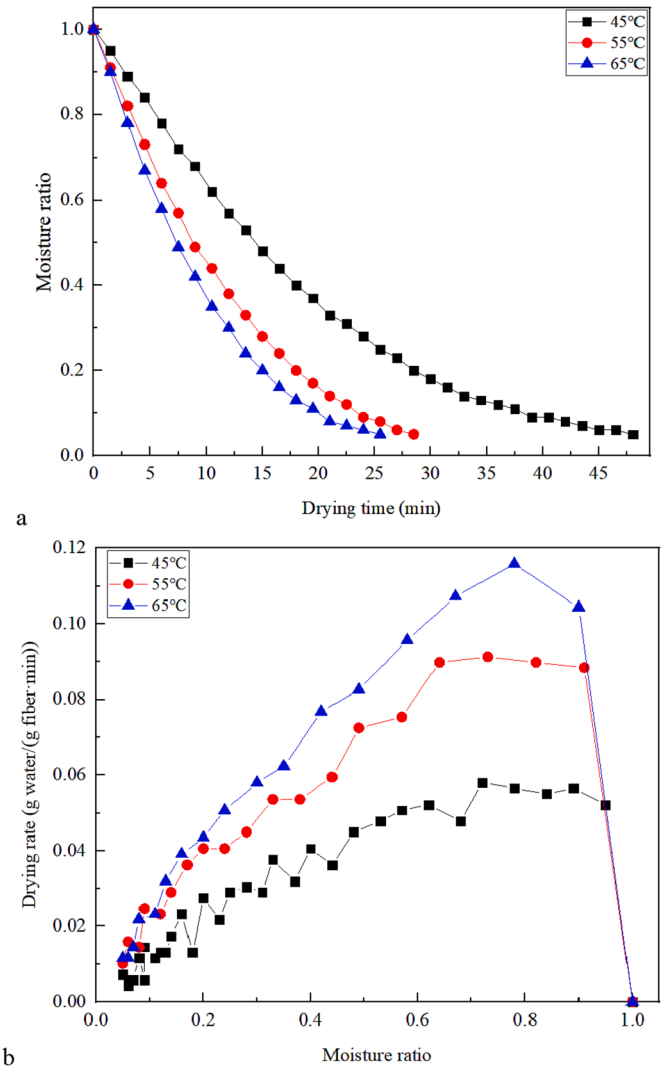

Fig. 2. a). Moisture ratio with drying time at different temperatures; b). Drying rate vs moisture ratio of pulp at different temperatures.

3.1.2. CD kinetic model

Table 2 shows the statistical analysis results for the six mathematical models in CD. The values of R^2 in all models were higher than 0.988, and the values of χ^2 and *RMSE* were lower than 0.0010 and 0.0311, respectively. In particular, the values of R^2 in Page models were higher than 0.999, and corresponding values of χ^2 and *RMSE* were lower than 5.0×10^{-4} and 0.0069 at all the selected temperatures. Thus, the Page model could be used to describe the pulp CD kinetics more accurately than the other models.

The accuracy of the kinetic model was verified by plotting the experimental and predicted moisture content. Fig. 3a shows the comparison of predicted and experimental moisture ratio of pulp dried at 45, 55, and 65 ℃ with the Page model. The statistical results were also presented in Fig. 3a, with R^2 above 0.999, χ^2 below 0.00005 and *RMSE* as low as 0.0023. It can be seen that the predicted values given by the Page model were almost identical with the experimental values.

3.1.3. Effective moisture diffusivity and activation energy of CD

The effective moisture diffusion (D_{eff}) at different temperatures can be obtained by Eq. (10) and the calculated results has been given in Table 3. It shows that D_{eff} was changed from 1.08×10^{-10} to 2.08×10^{-10} m^2/s in the CD process when the drying temperature increased from 45 to 65 ℃. As expected, the value of D_{eff} increases with drying temperature. This also indicates high temperature favors moisture-solid separation due to diffusivity enhancement.

The activation energy of CD ($E_{a,CD}$) was then calculated with Eq. (13). From the relationship of ln (D_{eff}) and $1/T$ for convective drying of pulp as given in Fig. 4a, the activation energy was found to be 29.6 kJ/mol for the dried pulp.

3.2. Ultrasound-assisted drying (UAD) results and discussion

3.2.1. Effect of ultrasonic power on UAD kinetics

The effect of ultrasonic power on pulp drying under the temperature of 55 ℃ has been given in Fig. 5a. As it displays, the drying time of the UAD was decreased to 21.0, 18.0, and 16.5 min at different ultrasonic powers. Compared with the CD process at the same drying temperature, the drying time was shortened by 26 %, 37 %, and 42 %, respectively. Therefore, UAD was able to speed up pulp drying significantly. Besides, the drying rate increases with the increase of ultrasonic power. This is mainly attributed to the mechanism that ultrasound reduces both external and internal moisture separation resistance from the pulp to the dry medium. The reduction of external resistance is explained by the fact that ultrasonic affects the diffusion boundary layer by introducing pressure change, oscillation velocity, and micro-flow at the interface of

Table 2
Statistical results of kinetic model for pulp convective drying.

Model	Temperature (℃)	Constants or coefficients				χ^2	*RMSE*	R^2
Lewis	45	$k = 0.00088$				0.0010	0.0311	0.988
	55	$k = 0.00141$				0.0010	0.0310	0.989
	65	$k = 0.00171$				0.0008	0.0276	0.991
Page	45	$k = 0.00020$	$n = 1.202$			0.00003	0.0056	1.000
	55	$k = 0.00037$	$n = 1.119$			0.00005	0.0069	0.999
	65	$k = 0.00052$	$n = 1.182$			0.00001	0.0023	1.000
Logarithmic	45	$k = 0.00076$	$a = 1.135$	$c = -0.104$		0.0002	0.0125	0.998
	55	$k = 0.00115$	$a = 1.141$	$c = -0.121$		0.0001	0.0098	0.999
	65	$k = 0.00150$	$a = 1.102$	$c = -0.075$		0.0002	0.0126	0.998
Henderson and Pabis	45	$k = 0.00097$	$a = 1.062$			0.0006	0.0230	0.994
	55	$k = 0.00147$	$a = 1.052$			0.0007	0.0249	0.993
	65	$k = 0.00180$	$a = 1.050$			0.0005	0.0218	0.995
Wang and Singh	45	$a = -0.00067$	$b = 1.24E-7$			0.00003	0.0056	0.999
	55	$a = -0.00107$	$b = 3.06E-7$			0.00005	0.0069	0.999
	65	$a = -0.00130$	$b = 4.41E-7$			0.00012	0.0103	0.999
Midilli et al.	45	$k = -0.008$	$n = 1.212$	$a = 0.992$	$b = -0.049$	0.00023	0.0143	0.998
	55	$k = -0.012$	$n = 1.251$	$a = 0.986$	$b = -0.075$	0.00022	0.0133	0.998
	65	$k = -0.017$	$n = 1.222$	$a = 0.980$	$b = -0.090$	0.00043	0.0183	0.996

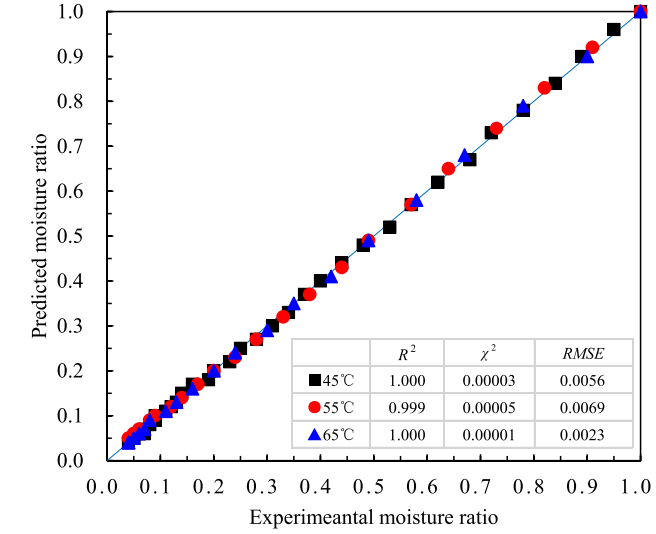

a

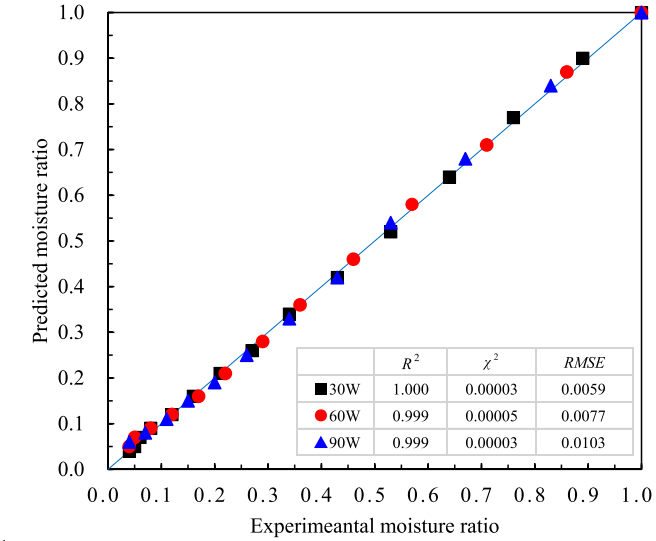

b

Fig. 3. a). Comparison of experimental and predicted moisture ratio of the Page model for pulp CD; b). Comparison of experimental and predicted moisture ratio of the Page model for pulp UAD.

Table 3
Effective moisture diffusivity and activation energy for convective and ultrasound-assisted drying of pulp.

Convective drying (CD)			Ultrasound-assisted drying (UAD)		
Temperature (℃)	D_{eff} (m^2/s)	$E_{a,CD}$ (kJ/mol)	P_{ug} (W)	D_{eff} (m^2/s)	$E_{a,UAD}$ (kJ/mol)
45	1.08×10^{-10}	29.6	30	2.77×10^{-10}	20.2
55	1.77×10^{-10}		60	3.06×10^{-10}	
65	2.08×10^{-10}		90	3.20×10^{-10}	

the material. The reduction of internal resistance could be caused by a series of rapidly alternating contractions and expansions (sponge effect) that leads to the formation of micro-channels in the pulp during the propagation of ultrasonic waves. Further, the high-intensity acoustic wave made the moisture in the fiber matrix cavitation, and the strong shear forces by cavitation also contribute to removing the moisture that was adsorbed by capillary forces in the pulp fiber network.

From the drying rate curves presented in Fig. 5b, the constant rate period did not exist for all the drying rate curves in UAD. A higher ultrasonic power could facilitate the drying rate at the initial drying stage, then the drying rate under different ultrasonic power showed a decreasing trend, approaching zero with moisture content changes of the pulp sample. At the initial drying period, the pulp can absorb a great amount of ultrasonic energy, which intensified the moisture separation process by the mechanical and cavitation effect. After approaching the maximum drying rate, the ultrasonic energy absorbed by the pulp decreased due to the increase of diffusion resistance; as a result, the drying rate begins to reduce accordingly. Liu et al. (2017) observed a similar phenomenon when investigated the strengthening effect of contact ultrasound on hot air drying of sweet potato. Compared to the convective drying rate shown in Fig. 2b, we found from Fig. 5b that the drying rate was enhanced by 49 % and 99 % under the ultrasonic power of 30 and 60 W, respectively. When the moisture content was reduced to half of the initial value, the drying rate was still enhanced by 40 % and 84 %. The drying rate of UAD was much higher than that of CD, thus UAD was able to intensify pulp convective drying process effectively.

To further understand the coupling relationship between ultrasonic power and moisture transport, three key points can offer more information in Fig. 4b. The first key point was observed when the *MR* was 0.90. All the drying curves showed the same drying rate and growth trend under various ultrasonic powers before the *MR* dropped to 0.90.

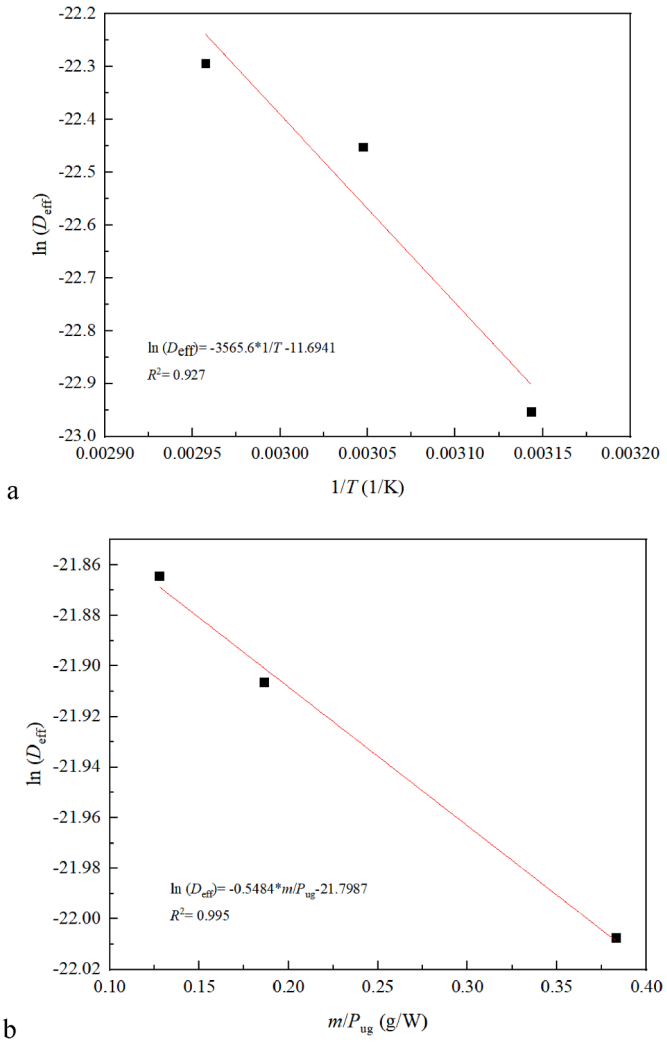

Fig. 4. a). Plot of ln (D_{eff}) versus 1/T for pulp CD; b). Plot of ln (D_{eff}) versus m/P_{ug} for pulp UAD.

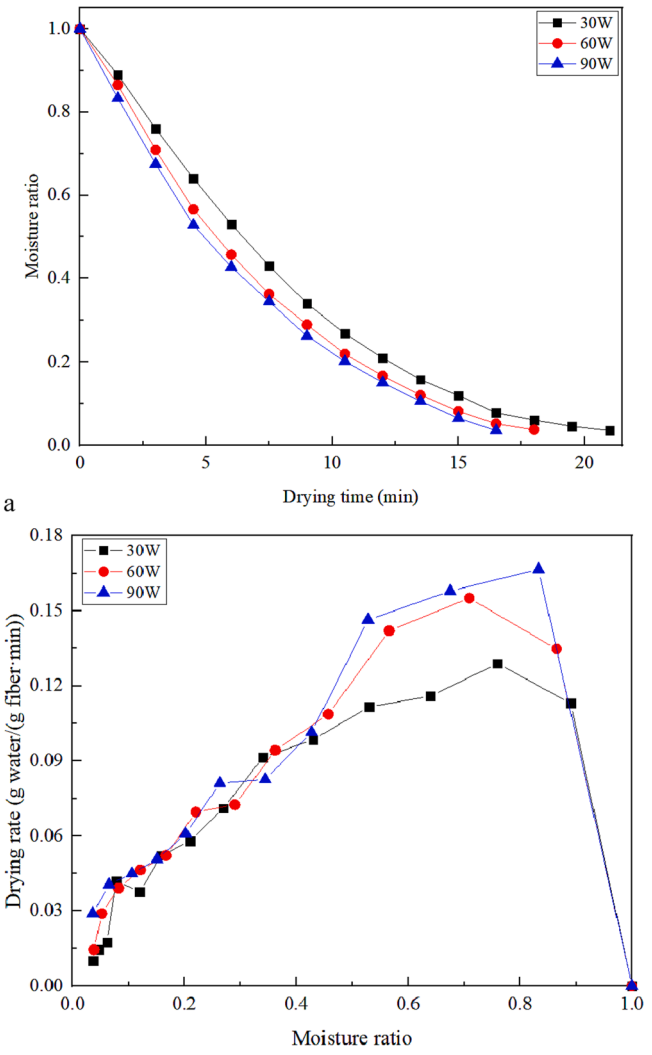

Fig. 5. a). Moisture ratio with drying time at different ultrasonic powers; b). Drying rate vs moisture ratio of pulp at different ultrasonic powers.

As the drying process progresses, the second key point emerged when the *MR* was 0.67. The two drying rate curves at 60 and 90 W were almost intersected and maintained a similar downward trend then, but the drying rates of both were much higher than that of dried at 30 W. When the *MR* of pulp reached 0.43, the last key point appeared. From then on, there was no sharp distinction among the three drying rate curves until the end of drying. This demonstrates that increasing ultrasonic power was not enhancing the drying rate or shorten the drying time when the *MR* was below 0.43 in the UAD process. It proved that there was a specific or threshold moisture content, below which there was no significant difference regarding the drying rate. Therefore, the drying performance and energy consumption could be improved further if variable ultrasonic powers were employed in different drying stages, which would be investigated in the future for pulp and paper products in the UAD process.

3.2.2. *UAD kinetic model*

The results of the statistical analysis of the six mathematical models in UAD are shown in Table 4. The R^2, χ^2, and *RMSE* were also used to determine the best-fitting model. From Table 4, the values of R^2 of all the kinetic models were higher than 0.982, and the values of χ^2 and *RMSE* were lower than 0.0019 and 0.0423, respectively. Among them, the values of R^2 from Page models were higher than 0.999, and the corresponding values of χ^2 and *RMSE* were lower than 0.0001 and 0.0103, respectively. Thus, as the models of CD, the Page model could also be used to describe the pulp UAD kinetics more accurately than the other models.

Fig. 3b presents the comparison of predicted and experimental moisture content in the UAD of pulp sample at ultrasonic power of 30, 60, and 90 W with the Page model. It can be seen that the predicted values by the Page model were quite consistent with the experimental values, and a straight line with slope 1 through the origin was presented in the figure. The statistical results were also presented in Fig. 3b, with R^2 above 0.999, χ^2 below 0.0001 and *RMSE* as low as 0.0059. It reveals that the Page model could describe and predict the drying kinetics in UAD.

3.2.3. *Effective moisture diffusivity and activation energy of UAD*

The effective moisture diffusivity (D_{eff}) was found to enhanced from 2.77×10^{-10} at 30 W to 3.20×10^{-10} m^2/s at 90 W in the UAD process as presented in Table 3. Compared with CD at the same drying temperature, the values of D_{eff} were increased by 56 %, 73 %, and 81 % under various ultrasonic powers. The improvement of moisture diffusivity also indicated UAD could facilitate moisture separation in the pulp drying process.

From the relationship of ln (D_{eff}) and m/P_{ug} for ultrasound-assisted drying of pulp as given in Fig. 4b, the activation energy of UAD ($E_{a,UAD}$) could be calculated with Eq. (14)-(16). The value of $E_{a,UAD}$ was found to be 20.2 kJ/mol in this work. It was reduced by 32 % compared

Table 4
Statistical results of kinetic model for pulp ultrasound-assisted drying.

Model	Ultrasonic power (W)	Constants or coefficients				χ^2	*RMSE*	R^2
Lewis	30	$k = 0.00203$				0.0019	0.0423	0.982
	60	$k = 0.00233$				0.0012	0.0336	0.988
	90	$k = 0.00249$				0.0007	0.0245	0.993
Page	30	$k = 0.00032$	$n = 1.293$			0.00008	0.0059	1.000
	60	$k = 0.00048$	$n = 1.219$			0.00009	0.0077	0.999
	90	$k = 0.00101$	$n = 1.147$			0.00010	0.0103	0.999
Logarithmic	30	$k = 0.00160$	$a = 1.180$	$c = -0.147$		0.0004	0.0178	0.997
	60	$k = 0.00185$	$a = 1.153$	$c = -0.133$		0.0001	0.0105	0.999
	90	$k = 0.00202$	$a = 1.118$	$c = -0.112$		0.00004	0.0043	1.000
Henderson and Pabis	30	$k = 0.00217$	$a = 1.067$			0.0014	0.0250	0.987
	60	$k = 0.00244$	$a = 1.050$			0.0009	0.0283	0.992
	90	$k = 0.00256$	$a = 1.030$			0.0006	0.0217	0.995
Wang and Singh	30	$a = -0.00153$	$b = 6.13E-7$			0.00008	0.0082	0.999
	60	$a = -0.00176$	$b = 8.14E-7$			0.00009	0.0088	0.999
	90	$a = -0.00190$	$b = 9.67E-7$			0.00030	0.0158	0.997
Midilli et al.	30	$k = -0.034$	$n = 1.102$	$a = 1.004$	$b = -0.124$	0.00064	0.0240	0.999
	60	$k = -0.023$	$n = 1.252$	$a = 0.991$	$b = -0.124$	0.00027	0.0158	0.997
	90	$k = -0.023$	$n = 1.272$	$a = 0.976$	$b = -0.128$	0.00016	0.0129	0.996

with CD process. Gamboa-Santos et al. (2014) reported similar results in the UAD process of strawberries, with the E_a values of 21.9 ± 2.1 kJ/mol and 20.6 ± 1.8 kJ/mol at the ultrasonic power of 30 and 60 W, respectively. The difference in E_a between CD and UAD indicated that the ultrasound-assisted drying method could conserve energy consumption in the traditional convective pulp drying process.

3.3. Comparative evaluation of energy consumption between CD and UAD

Fig. 6a presents the results of *TEC* in pulp drying process, calculated with Eq. (17). After intensifying the drying with UAD, the *TEC* was decreased to 0.31 kWh at the drying temperature of 45 ℃ compared with 0.53 kWh of CD, which means that 0.22 kWh of energy consumption could be saved, equivalent to 42 % of energy saving potential at the same drying temperature. The energy savings under the temperature of 55 and 65 ℃ were 0.11 and 0.08 kWh, respectively, accounting for 31 % and 22 % of *TEC* in the CD process. Compared with CD, the total energy consumption of UAD was reduced by 42 %~22 %. This indicates that energy savings tend to decrease with increasing drying temperature. However, it also noted that the CD at 55 ℃ and 65 ℃ consumes almost the same amount of *TEC*, but the UAD at 55 ℃ used less *TEC* than dried at 65 ℃. Thus, for maximizing energy savings with UAD, the pulp is recommended to be dried at 55 ℃.

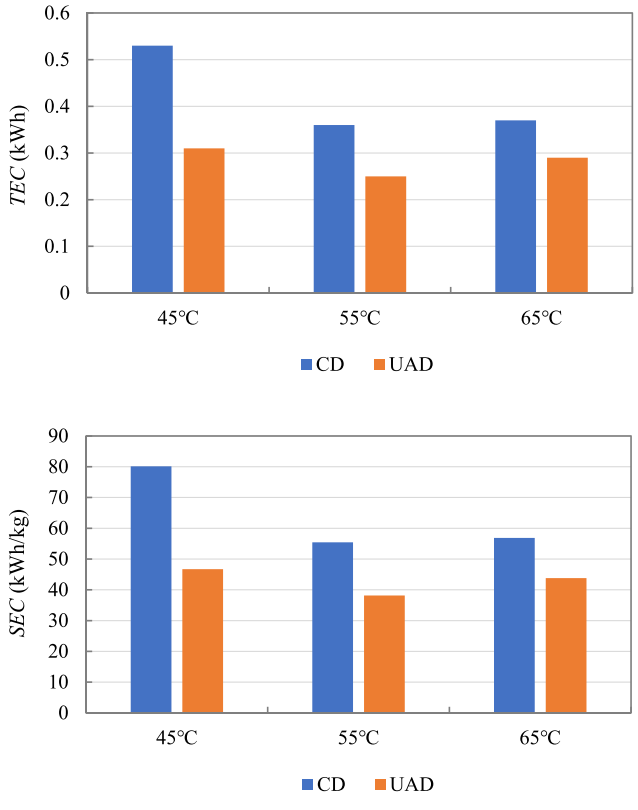

Fig. 6. a). Total energy consumption (*TEC*) of pulp drying process; b). Specific energy consumption (*SEC*) of pulp drying process.

The same saving results could also be observed with the *SEC* in the CD and UAD process, calculated with Eq. (18). As illustrated in Fig. 6b, the *SEC* was 80.12, 55.44, and 56.88 kWh/kg in the CD process. With UAD intensification, it was reduced to 46.73, 38.15, and 43.79 kWh/kg at the same drying temperatures. The results show that the specific energy consumption of UAD-dried pulp could be decreased significantly although additional power would be used by the ultrasonic generator. Through analysis of the specific energy consumption, we find that ultrasonic intensification at the temperature of 45 ℃ or 65 ℃ is not conducive to saving energy. It also demonstrated that more energy was saved at the drying temperature of 55 ℃. Thus, it could be concluded that UAD is an eco-friendly and efficient process requiring less time and energy consumption. Furthermore, the pulp drying process was suggested be operated at 55 ℃ with lower either *TEC* or *SEC* when enhanced by UAD. Additionally, the *SEC* could also be used to evaluate the energy efficiency under other temperatures and ultrasonic powers that were out of the ranges of this study, which will be investigated in the future for intensifying the pulp drying process further.

4. Conclusions

This study compared the drying behavior of pulp under CD and UAD showing the latter process to be faster and more efficient with 26 %~42 % drying time reductions and 42 %~22 % energy savings. High ultrasonic power was not always beneficial to enhance moisture separation when MR decreased to 0.43. Although the constant rate period was not observed in UAD, the minimized energy consumption was obtained at 55 °C and 60 W. The Page model was found to best predict the pulp drying kinetics for both methods. Thus, UAD could be used to intensify moisture separation in the pulp drying process effectively.

CRediT authorship contribution statement

Lingbo Kong: Conceptualization, Investigation, Methodology, Writing – original draft, Writing – review & editing. **Jiahao Li:** Data

curation, Investigation, Visualization, Writing – original draft. **Wolfgang Eichhammer:** Supervision, Writing – review & editing.

Declaration of competing interest

The authors declare that they have no known competing financial interests or personal relationships that could have appeared to influence the work reported in this paper.

Data availability

Data will be made available on request.

Acknowledgements

This work was supported by the Scientific Research Program Funded by Education Department of Shaanxi Provincial Government (Program No. 23JP013).

References

Asar, M.E., Noori, Z., Yagoobi, J., 2022. Numerical investigation of the effect of ultrasound on paper drying. TAPPI J. 21 (3), 127–140.
Behera, B., Balasubramanian, P., 2021. Experimental and modelling studies of convective and microwave drying kinetics for microalgae. Bioresour. Technol. 340, 125721.
Beigi, M., Torki, M., 2021. Experimental and ANN modeling study on microwave dried onion slices. Heat Mass Transfer 57 (5), 787–796.
Buzrul, S., 2022. Reassessment of thin-layer drying models for foods: A critical short communication. Processes 10 (1), 118.
Cárcel, J.A., Benedito, J., Rosselló, C., Mulet, A., 2007. Influence of ultrasound intensity on mass transfer in apple immersed in a sucrose solution. J. Food Eng. 78 (2), 472–479.
Dupuis, E.D., Momen, A.M., Patel, V.K., Shahab, S., 2019. Electroelastic investigation of drying rate in the direct contact ultrasonic fabric dewatering process. Appl. Energy 235, 451–462.
Ertekin, C., Firat, M., 2015. A comprehensive review of thin-layer drying models used in agricultural products. Crit. Rev. Food Sci. Nutr. 57 (4), 701–717.
Fan, K., Zhang, M., Mujumdar, A.S., 2017. Application of airborne ultrasound in the convective drying of fruits and vegetables: A review. Ultrason. Sonochem. 39, 47–57.
Gamboa-Santos, J., Montilla, A., Cárcel, J.A., Villamiel, M., Garcia-Perez, J.V., 2014. Air-borne ultrasound application in the convective drying of strawberry. J. Food Eng. 128, 132–139.
García-Pérez, J.V., Cárcel, J.A., Riera, E., Mulet, A., 2009. Influence of the applied acoustic energy on the drying of carrots and lemon Peel. Drying Technol. 27 (2), 281–287.
Huang, D., Men, K., Li, D., Wen, T., Gong, Z., Sunden, B., Wu, Z., 2020. Application of ultrasound technology in the drying of food products. Ultrason. Sonochem. 63, 104950.
Huang, D., Yang, P., Tang, X., Luo, L., Sunden, B., 2021. Application of infrared radiation in the drying of food products. Trends Food Sci. Technol. 110, 765–777.
Kowalski, S.J., Mierzwa, D., 2015. US-assisted convective drying of biological materials. Drying Technol. 33 (13), 1601–1613.
Li, P., Chen, Z., 2017. Experiment study on porous fiber drying enhancement with application of power ultrasound. Appl. Acoust. 127, 169–174.
Liu, Y., Sun, Y., Yu, H., Yin, Y., Li, X., Duan, X., 2017. Hot air drying of purple-fleshed sweet potato with contact ultrasound assistance. Drying Technol. 35 (5), 564–576.
Luo, D.L., Liu, J., Liu, Y.H., Ren, G.Y., 2015. Drying characteristics and mathematical model of ultrasound assisted hot-air drying of carrots. Int. J. Agric. Biol. Eng. 8 (4), 124–132.
O'Connor, Z.N., Yagoobi, J.S., Tilley, B.S., 2023. Experimental study of paper drying with direct-contact ultrasound mechanism. Drying Technol. 41 (8), 1351–1364.
Onwude, D.I., Hashim, N., Janius, R.B., Nawi, N.M., Abdan, K., 2016. Modeling the thin-layer drying of fruits and vegetables: A review. Compr. Rev. Food Sci. Food Saf. 15 (3), 599–618.
Ozuna, C., Gómez Álvarez-Arenas, T., Riera, E., Cárcel, J.A., Garcia-Perez, J.V., 2014. Influence of material structure on air-borne ultrasonic application in drying. Ultrason. Sonochem. 21 (3), 1235–1243.
Peng, C., Moghaddam, S., 2021. Experimental evaluation and kinetic analysis of direct-contact ultrasonic fabric drying process. J. Therm. Sci. Eng. Appl. 13 (2), 021025.
Peng, C., Momen, A.M., Moghaddam, S., 2017a. An energy-efficient method for direct-contact ultrasonic cloth drying. Energy 138, 133–138.
Peng, C., Ravi, S., Patel, V.K., Momen, A.M., Moghaddam, S., 2017b. Physics of direct-contact ultrasonic cloth drying process. Energy 125, 498–508.
Siucińska, K., Konopacka, D., 2014. Application of ultrasound to modify and improve dried fruit and vegetable tissue: A review. Drying Technol. 32 (11), 1360–1368.
Sun, G.Y., Chen, M.Q., Huang, Y.W., 2017. Evaluation on the air-borne ultrasound-assisted hot air convection thin-layer drying performance of municipal sewage sludge. Ultrason. Sonochem. 34, 588–599.
Tayyab Rashid, M., Liu, K., Ahmed Jatoi, M., Safdar, B., Lv, D., Wei, D., 2022. Developing ultrasound-assisted hot-air and infrared drying technology for sweet potatoes. Ultrason. Sonochem. 86, 106047.
Yang, M., Yagoobi, J., 2022. Enhancement of drying rate of moist porous media with dielectrophoresis mechanism. Drying Technol. 40 (14), 2952–2963.
Yao, Y., Pan, Y., Liu, S., 2020. Power ultrasound and its applications: A state-of-the-art review. Ultrason. Sonochem. 62, 104722.
Zhang, Y., Abatzoglou, N., 2020. Review: Fundamentals, applications and potentials of ultrasound-assisted drying. Chem. Eng. Res. Des. 154, 21–46.
Zhang, D., Huang, D., Zhang, Y., Lu, Y., Huang, S., Gong, G., Li, L., 2023. Ultrasonic assisted far infrared drying characteristics and energy consumption of ginger slices. Ultrason. Sonochem. 92, 106287.
Zhu, X., Zhang, Z., Hinds, L.M., Sun, D.-W., Tiwari, B.K., 2021. Applications of ultrasound to enhance fluidized bed drying of Ascophyllum Nodosum: Drying kinetics and product quality assessment. Ultrason. Sonochem. 70, 105298.